JACS
JOURNAL OF THE AMERICAN CHEMICAL SOCIETY
Article
Cite This: J. Am. Chem. Soc. 2019, 141, 17937−17948
pubs.acs.org/JACS

Mechanism of Ni-Catalyzed Reductive 1,2-Dicarbofunctionalization of Alkenes

Qiao Lin and Tianning Diao*

Department of Chemistry, New York University, 100 Washington Square East, New York, New York 10003, United States

Supporting Information

ABSTRACT: Ni-catalyzed cross-electrophile coupling reactions have emerged as appealing methods to construct organic molecules without the use of stoichiometric organometallic reagents. The mechanisms are complex: plausible pathways, such as "radical chain" and "sequential reduction" mechanisms, are dependent on the sequence of the activation of electrophiles. A combination of kinetic, spectroscopic, and organometallic studies reveals that a Ni-catalyzed, reductive 1,2-dicarbofunctionalization of alkenes proceeds through a "sequential reduction" pathway. The reduction of Ni by Zn is the turnover-limiting step, consistent with Ni(II) intermediates as the catalyst resting-state. Zn is only sufficient to reduce (phen)Ni(II) to a Ni(I) species. As a result, commonly proposed Ni(0) intermediates are absent under these conditions. (Phen)Ni(I)−Br selectively activates aryl bromides via two-electron oxidation addition, whereas alkyl bromides are activated by (phen)Ni(I)−Ar through single-electron activation to afford radicals. These findings could provide insight into achieving selectivity between different electrophiles.

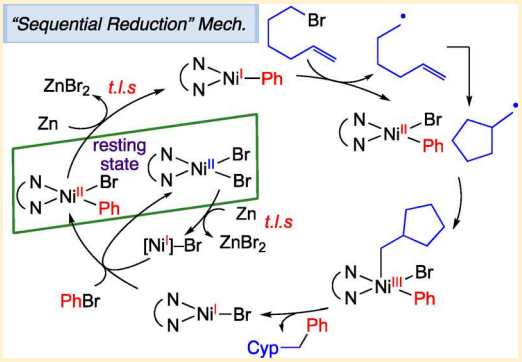

INTRODUCTION

Nickel-catalyzed cross-coupling reactions have presented as powerful methods for constructing organic molecules.[1] Cross-electrophile coupling reactions, under reductive conditions, can bypass the need for pregenerated, air-sensitive organometallic reagents, and thus improve reaction scope and functional group compatibility.[2] Understanding the mechanisms of Ni-catalyzed cross-coupling reactions could inform the design of catalysts and the control of selectivity, but there are challenges due to the diversity of possible pathways and the complexity of electronic structures of multivalent Ni intermediates.[3] Since the seminal study of $Ni(PPh_3)_4$ by Kochi,[4] contemporary work has focused on modern systems with bidentate and tridentate ligands,[5,6] the mechanisms of which appear to be system-dependent. While (NHC)Ni catalysts lead to two-electron redox processes mediated by Ni(0)/Ni(II) intermediates,[6] catalysts with chelating ligands often involve radical pathways going through Ni(0)/Ni(I)/Ni(II)/Ni(III) intermediates.[5]

Previous efforts to characterize the mechanisms of Ni-catalyzed cross-electrophile coupling reactions leave several key questions unanswered. Evidence for distinguishing "radical chain" from "sequential reduction" pathways remains ambiguous (Scheme 1).[5l] These two pathways differ by the sequence of activations of Csp^2 and Csp^3 electrophiles, which are critical for achieving chemoselectivity in cross-electrophile coupling reactions.[2] Moreover, despite recent, rigorous efforts in characterizing paramagnetic Ni reaction intermediates,[7] the identity of the catalyst resting-state in a catalytic reaction with *N*-ligands has rarely been characterized.[5h−n] Finally, previous studies have identified the reduction of the Ni catalyst as the turnover-limiting step,[5l,8] but ambiguity remains in the structural characterization of the resulting Ni species.

Reductive alkene carbofunctionalization with electrophiles has found widespread utility.[9] We recently developed a Ni-catalyzed, reductive, two-component 1,2-dicarbofunctionalization of alkenes (Scheme 1).[10,11] This reaction exhibits a broad scope and is compatible with a large variety of functional groups, allowing access to important pyrrolidine and piperidine derivatives. The combination of $NiBr_2$·DME with 1,10-phenanthroline (phen) in DMA (*N*,*N*-dimethylacetamide) as the solvent, and Zn as the reductant, represents common conditions for reductive cross-coupling reactions.[8,12] "Radical chain"[5m,n] and "sequential reduction"[13] pathways are both plausible (Scheme 1), based on recent mechanistic studies. "Radical chain" mechanisms (cycles A and B) feature the activation of alkyl halides by (phen)Ni(I)Br to form a radical (step i), which then combines with the reduced Ni species. In cycle A, radicals combine with Ni(0) (step iii) followed by oxidative addition of PhBr (step iv); in cycle B, oxidative addition of PhBr (step vi) takes place prior to radical combination with Ni(II) (step vii). The alternative "sequential reduction" mechanism, cycle C, reverses the sequence of electrophile activation in the "radical chain" mechanism. Oxidative addition of PhBr to Ni(0) affords Ni(II)(Ph)(Br) (step vi), followed by the reduction of Ni(II) to form Ni(I)−Ph (step viii). Activation of the alkyl bromide by Ni(I)−Ph

Received: September 16, 2019
Published: October 7, 2019

DOI: 10.1021/jacs.9b10026
J. Am. Chem. Soc. 2019, 141, 17937−17948

Scheme 1. Ni-Catalyzed Reductive 1,2-Dicarbofunctionalization of Alkenes and Possible Mechanisms

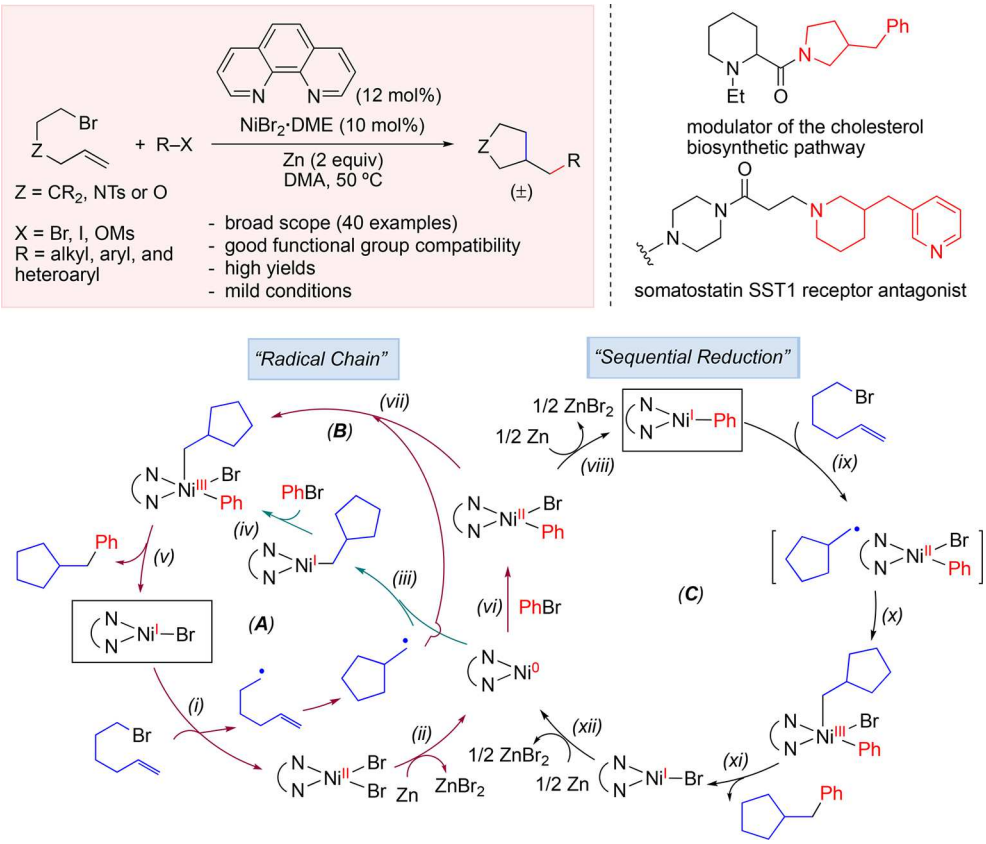

generates a radical (step ix), which combines with Ni(II) to form a Ni(III) intermediate (step x).[14]

Herein, we report a mechanistic study on the reductive 1,2-dicarbofunctionalization reaction. Kinetic studies, in combination with the characterization of reaction intermediates, differentiate the "radical chain" pathways from the "sequential reduction" mechanism. In addition, our results answer several critical questions, including the identity of the turnover-limiting step and the catalyst resting-state, the nature of the interaction between Ni and Zn, and the sequence of activation of different electrophiles. These data highlight the importance of the catalyst reduction step, and elucidate the mechanistic attributes behind the selectivity achieved in cross-electrophile coupling reactions.

RESULTS AND DISCUSSION

Substrate Probes. Substrate probes were subjected to the standard reaction conditions, $NiBr_2$·DME in combination with 1,10-phenanthroline and Zn in DMA (*N*,*N*-dimethylacetamide) at 50 °C, to ascertain the presence of radical intermediates. The coupling of **1** with PhBr afforded dimer **4** in 8% yield under standard conditions (Scheme 2A).[10] Replacing 1,10-phenanthroline with the bulkier neocuproine increased the yield of **4** to 30%. Both *cis*- and *trans*-**5** proceeded to give the same mixture of *cis*- and *trans*-**6** in a ratio of 1:1.6 (Scheme 2B). Radical clock substrates **7** and **9** underwent cyclopropyl ring-opening upon cross-coupling, to afford products **8** and **10**, respectively (Scheme 2C).

These data provide evidence for the formation of radicals upon activation of alkyl bromides. Product **4**, resulting from the dimerization of **1**, is a common indication of radical intermediates.[15] Although the C−C bond formed in **4** could have also arisen from reductive elimination from a dialkyl Ni species, the increased yield of **4** with bulkier neocuproine suggests that the formation of **4** does not involve metal and competes with the Ni-mediated pathway to generate **2**. The convergence of the stereocenter for *cis*- and *trans*-**5** upon cyclization is consistent with formation of a radical intermediate erasing the substrate stereoinformation. The poor diastereoselectivity reflects a small energy difference in the chair and boat conformations in the transition states of cyclization,[16] and is consistent with the stereo-outcome of previous radical cyclizations initiated by tin hydride.[17] The ring-opening of the cyclopropyl groups of **7** and **9** implies that radical intermediates are formed at the C1 position of **7** and the C5 position of **9**.

Kinetic Studies. We carried out kinetic studies for the coupling of **11** with PhBr to form **12** as the model reaction, to resolve the orders of each reactant (eq 1). Reactions were

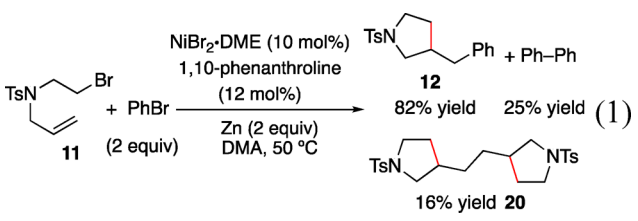

monitored by analyzing aliquots of the reaction mixture with GC. The decays of **11**, starting at two different concentrations, were compared to establish the catalyst's robustness using reaction progress kinetic analysis (RPKA) (Figure 1).[18] The time courses of two experiments, starting from different

DOI: 10.1021/jacs.9b10026
J. Am. Chem. Soc. 2019, 141, 17937−17948

Scheme 2. Substrate Probes for Determining Radical Intermediates

(A) Dimer Formation

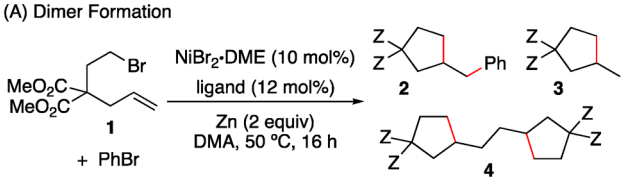

Ligand	2 (%yield)	3 (%yield)	4 (%yield)
1,10-phenanthroline	91	0	8
neocuproine	19	6	30

(B) Stereochemistry of Cyclization

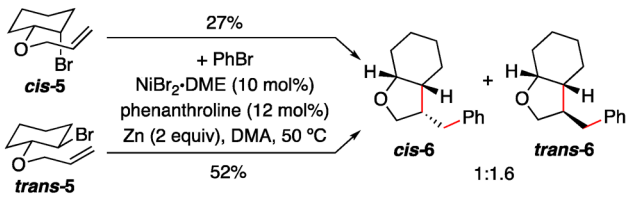

(C) Radical Clock

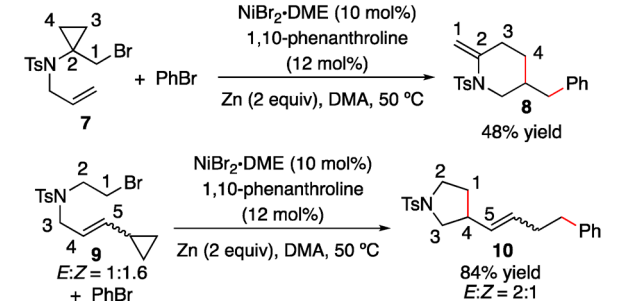

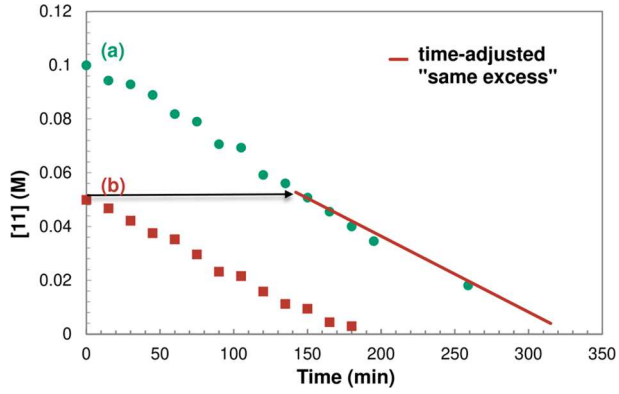

Figure 1. "Same-excess" experiment for alkene 1,2-dicarbofunctionalization shown in eq 1 with [excess] = $[PhBr]_0 - [\mathbf{11}]_0$ = 0.05 M. Reaction conditions: $[NiBr_2 \cdot DME]$ = 5 mM, [1,10-phenanthroline] = 6 mM, Zn = 0.1 mmol, solvent = DMA, agitation rate = 850 rpm; (a) $[\mathbf{11}]_0$ = 0.1 M; $[PhBr]_0$ = 0.15 M; (b) $[\mathbf{11}]_0$ = 0.05 M; $[PhBr]_0$ = 0.1 M.

substrate concentrations, fully overlay when the time was adjusted as the two reactions proceed under identical substrate concentrations onward from the point of intersection of the arrows. This result indicates that neither catalyst decomposition nor product inhibition took place over extended turnovers.

The time-courses for the reaction shown in eq 1 reveal that the decay of **11** and formation of **12** both fit a linear function (Figure 2A). The formation of the side-product, biphenyl, appears to be dependent on [PhBr]. "Different excess" experiments reveal that the formation of **12** overlays with the timecourse when starting at different [**11**] and [PhBr] at agitation rates of 900 and 1200 rpm, suggesting a zero-order dependence on [**11**] and [PhBr] (Figure 2B and C). A series of experiments with different [Ni] were performed to evaluate the order of [Ni]. Plotting the data according to variable time normalization analysis reveals that the power law order in [Ni] is 1 (Figure 2D).[19] Attempts to fit the data with other possible orders of [Ni] resulted in poor overlay of the time-courses (Figure S6). The "different excess" experiments allow us to estimate the k_{obs} values to be 8.6×10^{-4} and 12×10^{-4} s^{-1}, at 900 and 1200 rpm, respectively.

The presence of heterogeneous Zn prompted us to assess mass-transfer limitations.[20] Reactions were mixed in a shaker with orbital agitation. The reaction rate increases with increasing agitation speed (Figure 3A), but this rate acceleration plateaus when agitation rates exceed 1200 rpm. At a fixed agitation rate of 900 rpm, the reaction rate increases as Zn loading increases (Figure 3B). The use of larger particle size Zn dust reduces the rate as compared to fine Zn powder. Tetrabutylammonium iodide (TBAI) is known to facilitate heterogeneous reduction,[21] and addition of 10% TBAI indeed accelerated the reaction (Table S2).

The lack of kinetic dependence on substrates and first-order dependence on [Ni] and the observed rate dependence on the mixing speed and Zn loading reveal that the reduction of Ni by Zn is the turnover-limiting step. The reduction is expected to occur in two steps: mass-transfer when Ni is adsorbed to the surface of Zn, followed by electron-transfer from Zn to Ni.[22] The reduction is dependent on several factors, including convective transfer rate, electron transfer rate, and available surface area. Increasing the mixing speed to 1200 rpm leads to an increase in rate due to enhanced convective mass transfer. At agitation speeds greater than 1200 rpm, the effect of enhanced mass transfer is saturated and results in no further acceleration. In this scenario, the limiting factor becomes electron transfer on the Zn surface. The rate is proportional to the density of available surface area. Higher Zn loading increases the overall surface area, and thus the reaction rate.

Collectively, the rate law for the 1,2-dicarbofunctionalization of alkenes is expressed in eq 2. The zero-order dependence on organic substrates reveals that neither olefin **11** nor PhBr participates in the turnover-limiting step. The combination of the first-order dependence on [Ni] and the rate enhancement by increasing mixing speed and Zn loading suggests that the reduction of Ni by Zn is the rate-determining step. The power-law order of Zn is dependent on the distribution of Zn powder in solution.

$$\text{rate} = k_{obs}[\text{olefin}]^0[PhBr]^0[Ni][Zn]^x \quad (2)$$

Spectroscopic Characterization of the Catalyst Resting State. We then probed the identity of the catalyst resting state through EPR, ^{1}H NMR, and UV−visible spectroscopy. An aliquot of the catalytic reaction mixture of eq 1 was withdrawn after reacting for 30 min, immediately frozen, and analyzed by EPR spectroscopy at 10 K, only to show the absence of an EPR signal. Performing the reaction shown in eq 3 under standard conditions in DMA-d_9 allowed us to take a snapshot of the catalyst resting-state using ^{1}H NMR spectros-

DOI: 10.1021/jacs.9b10026
J. Am. Chem. Soc. 2019, 141, 17937−17948

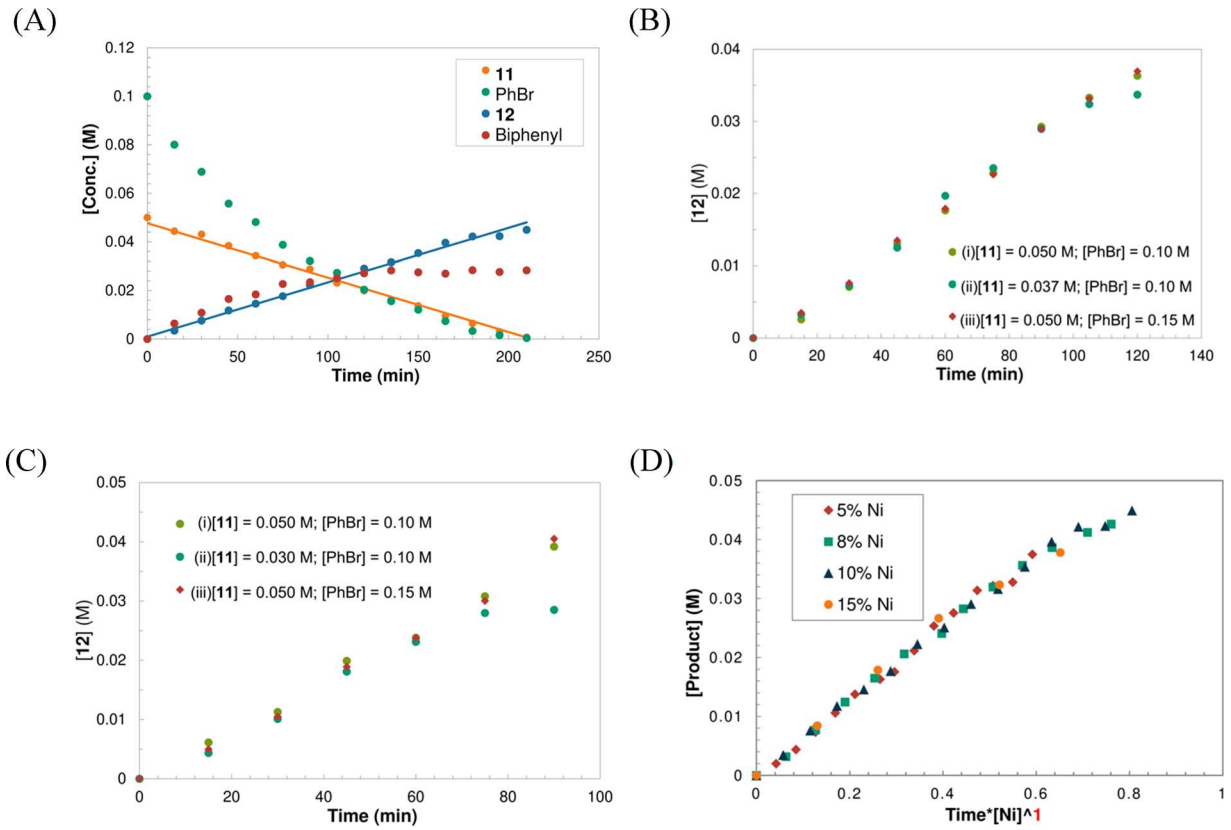

Figure 2. (A) Time-courses of the alkene 1,2-dicarbofunctionalization reaction shown in eq 1. Reaction conditions: $[\mathbf{11}]_0$ = 0.05 M, $[PhBr]_0$ = 0.1 M, $[NiBr_2{\cdot}DME]$ = 5 mM, [phen] = 6 mM, Zn = 0.1 mmol, solvent = DMA, agitation rate = 850 rpm. (B) "Different excess" experiments for determining the substrate orders at an agitation rate of 900 rpm. (C) "Different excess" experiments for determining the substrate orders at an agitation rate of 1200 rpm. (D) Determining [Ni] order based on the variable time normalization analysis, $[(phen)NiBr_2{\cdot}DME]$ = 2.5, 4, 5, 7.5 mM.

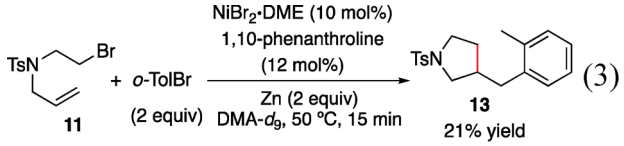

copy. After 15 min, the reaction was cooled to room temperature, filtered to remove Zn, and analyzed by ^{1}H NMR spectroscopy (Figure S17). Two Ni species are present: a paramagnetic species featuring broad resonances at 25.5 and 18.0 ppm and a diamagnetic species showing a group of downfield aromatic peaks (Figure 4C). Independently prepared $(phen)NiBr_2$ exhibits a group of paramagnetic peaks around 25.5 and 18.0 ppm identical to the paramagnetic resonances observed in the reaction mixture (Figure 4A).[23] Independently prepared (phen)Ni(*o*-Tol)(Br), made by mixing $Ni(cod)_2$ with phen and *o*-Tol-Br,[24] exhibits a set of diamagnetic peaks between 9.5 and 7.0 ppm, which is consistent with the diamagnetic species observed in the reaction mixture (Figure 4B). The ratio of $[(phen)NiBr_2]$ to [(phen)Ni(*o*-Tol)(Br)] is estimated to be 0.7:1. When (phen)Ni(*o*-Tol)(Br) was used as the precatalyst in place of $NiBr_2{\cdot}DME$, an analogous mixture of $(phen)NiBr_2$ and (phen)Ni(*o*-Tol)(Br) was observed at 25% conversion (Figure S17-2). Performing the same NMR experiments for the reaction shown in eq 1 resulted in identical paramagnetic resonances, but the intensity of the diamagnetic species was attenuated (Figures S18 and S19). We attribute this to the instability of (phen)Ni(Ph)(Br), which also underwent rapid decomposition during independent synthesis.

The UV−visible spectrum of the reaction mixture from eq 1 exhibits two absorptions at 421 and 456 nm, matching with the absorption spectrum of (phen)Ni(Ph)(Br) **16** (Figure 5). The reduction of $(phen)NiBr_2$ by Zn gives a purple solution, displaying a strong, distinct absorption at 565 nm. Addition of PhBr to this purple mixture resulted in a red solution with absorptions at 421 and 456 nm, consistent with the spectrum of (phen)Ni(Ph)(Br) **16**, as well.

The ^{1}H NMR data of the reaction mixture and the comparison with independently prepared complexes led us to assign the catalyst resting-state as a mixture of $(phen)NiBr_2$ and (phen)Ni(Ar)Br in a ratio of 0.7:1. This assignment is consistent with the lack of an EPR signal for this species and the reduction of Ni by Zn as the turnover-limiting step, as determined by kinetics. The UV−visible spectrum of the reaction mixture is identical to that of (phen)Ni(Ph)Br **16** because $(phen)NiBr_2$ does not display any strong absorption in the measured region. The "addition mixture" (Figure 5C), prepared by reduction of $(phen)NiBr_2$ by Zn followed by addition of PhBr, resembles the reaction mixture in their UV−visible spectra, suggesting that the catalyst resting-state could result from such a sequence of reactions.

Reduction of Ni by Zn, Characterized by Spectroscopy and Cyclic Voltammetry. Because the reduction of Ni by Zn was identified to be the turnover-limiting step, our subsequent study sought to closely characterize the reduced Ni

DOI: 10.1021/jacs.9b10026
J. Am. Chem. Soc. 2019, 141, 17937−17948

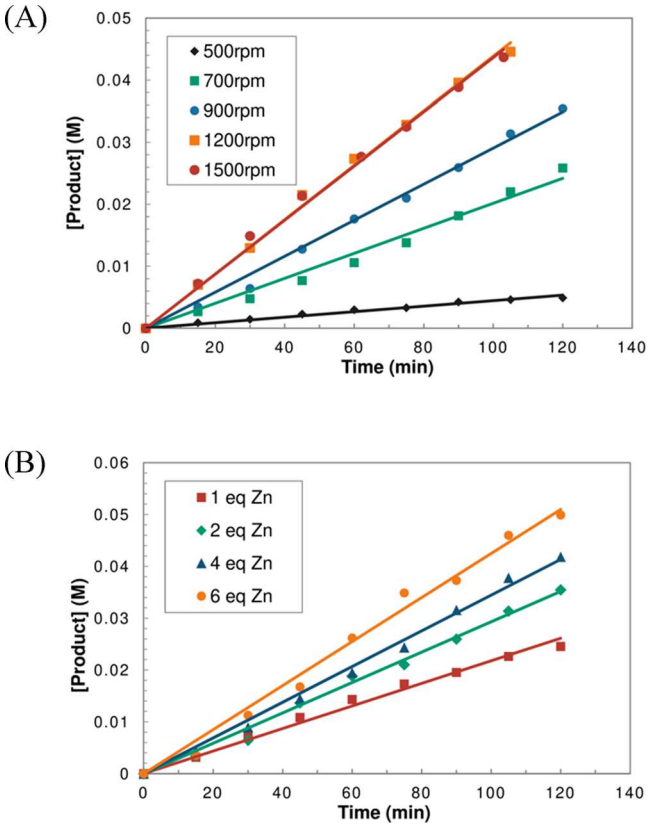

Figure 3. Formation of **12** over time under conditions identical to those shown in Figure 2A, except with different mixing speeds (A) and Zn loading (B).

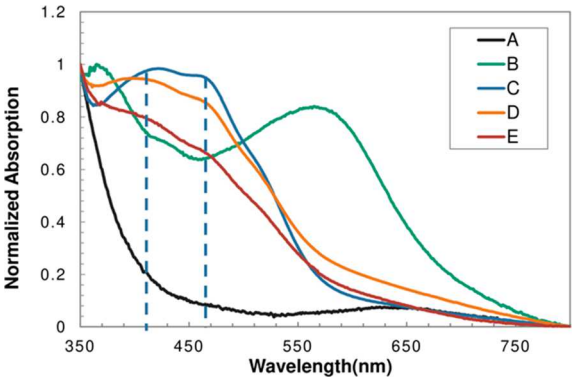

Figure 5. UV−visible spectra of (phen)$NiBr_2$ (A), (phen)$NiBr_2$ reduced by Zn (B), (phen)$NiBr_2$ reduced by Zn followed by addition of PhBr (C), (phen)Ni(Ph)(Br) **16** (D), and reaction mixture from eq 1 after 30 min (E).

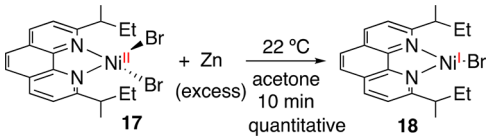

species, although previous investigations assign Ni(0) as the resulting species.[5l,8] Synthesis of model complex (phen*)$NiBr_2$ **17** (phen* = 2,9-di-*sec*-butyl-phenanthroline) allows us to isolate the reduction product, in which the Ni center is protected with the bulky phen* ligand. Treating **17** with excess Zn at room temperature generates a dark blue complex **18** in quantitative yield (eq 4). Single-crystal X-ray diffraction established the structure of **18** to be (phen*)Ni(I)Br (Figure 6A). The spin-density plot obtained from DFT calculations using the ORCA package revealed that the unpaired electron is located primarily on Ni (Figure 6B).[25] This result is corroborated by the EPR spectrum of **18**, which exhibits an axial signal (Figure 6C). No hyperfine splitting was resolved, probably due to small coupling constants.

Stirring the pale green (phen)$NiBr_2$ with excess Zn in DMA resulted in a dark purple solution **19**, which displays a series of paramagnetic ^{1}H NMR resonances (Figure S61) and an axial EPR signal (Figure 7). The integration of this EPR signal, quantified by comparison to an external standard, accounts for 10% of the starting Ni species. This purple species, however, is prone to decomposition, which hindered further characterization.

We then investigated the reduction potentials of relevant Ni species (Table 1). Data shown in Table 1 suggest that Zn can reduce Ni(II) complexes **14**, **16**, and **17** to Ni(I) species, but the reduction potential of −1.37 (V vs SHE) for (phen*)Ni(I)Br **18** implies that Zn is not sufficiently reducing to produce (phen)Ni(0) species via outer-sphere electron transfer.

The quantitative conversion of **17** to (phen*)Ni(I)Br **18**, upon Zn reduction, is corroborated with the lower reduction

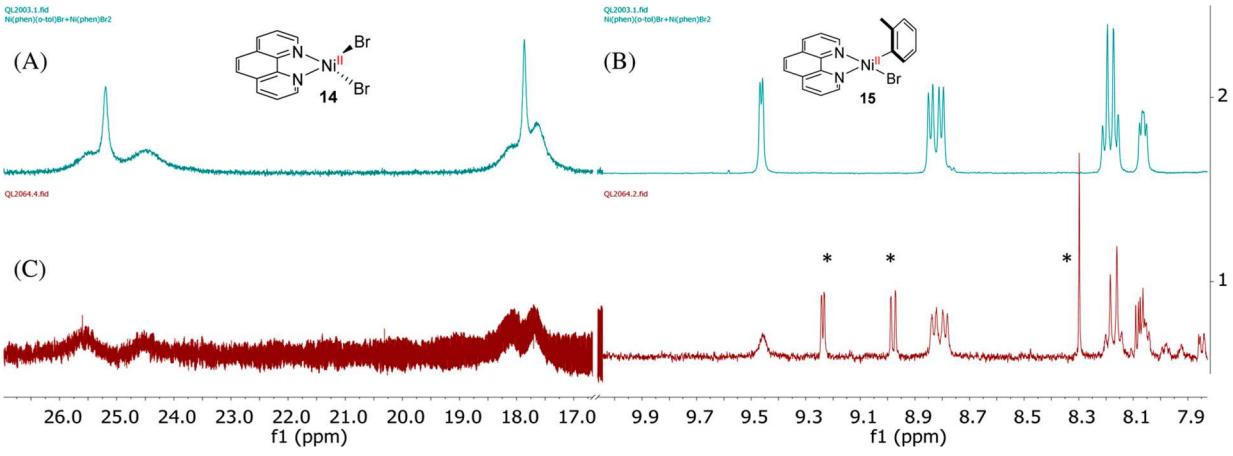

Figure 4. (A) ^{1}H NMR spectra of (phen)$NiBr_2$ **14** and (B) (phen)Ni(*o*-Tol)Br **15**; and (C) paramagnetic and diamagnetic regions of the reaction mixture shown in eq 3 under standard conditions. Solvent = DMA-d_9, * = uncoordinated 1,10-phenanthroline.

DOI: 10.1021/jacs.9b10026
J. Am. Chem. Soc. 2019, 141, 17937−17948

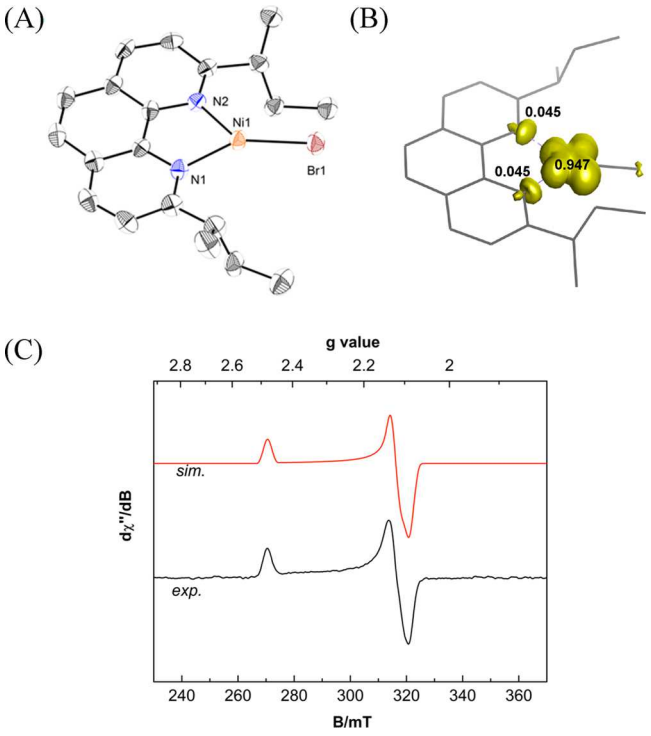

Figure 6. (A) X-ray crystal structure of Ni(phen*)Br **18** at 50% probability thermal ellipsoids. Hydrogen atoms are omitted for clarity. Selected bond lengths (Å): Ni(1)−Br(1)= 2.2879(8), Ni(1)−N(1) = 1.969(4), Ni(1)−N(2) = 1.968(4). (B) Spin-density plot based on DFT calculations. (C) X-Band EPR spectrum of complex **18**. Temperature = 10 K, solvent = toluene. Microwave frequency = 9.380 GHz, power = 0.02 mW, modulation amplitude = 1 mT/100 kHz, g = [2.4777, 2.1203, 2.0872].

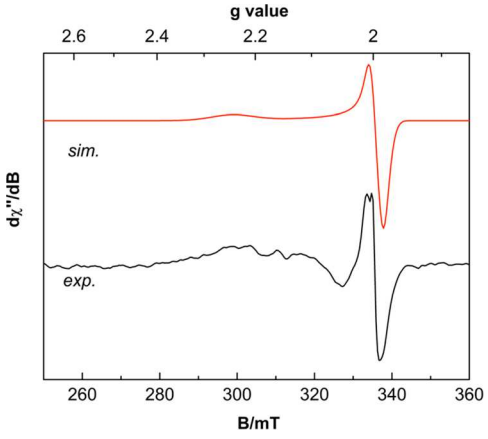

Figure 7. X-Band EPR spectrum of complex **19**. Temperature = 10 K, solvent = DMA. Microwave frequency = 9.380 GHz, power = 2.0 mW, modulation amplitude = 1 mT/100 kHz, g = [2.247, 1.993, 1.986].

potential of **18**, relative to Zn, indicating that Zn is insufficient to reduce **17** to a (phen*)Ni(0) state. Although phen* lacks catalytic reactivity due to its steric hindrance, its structural and electronic similarity to phen allows us to assign the structure of **19** by comparing its CV and EPR data with those of **18**. The paramagnetic ^{1}H NMR spectrum of **19** (Figure S61) is inconsistent with formation of d^{10} Ni(0) species. Comparing the CV of **14** with **17** reveals similar reduction potentials, which suggests that the reduction of (phen)NiBr$_2$ **14** likely

Table 1. Reduction Potentials of Ni Complexes and Comparison with Zn

complexes	$E_{p/2}$(Ni^{II}/Ni^{I}) (V vs SHE)	$E_{p/2}$((Ni^{I}/Ni^{0}) (V vs SHE)
(phen)NiBr$_2$ **14**	−0.86[a]	
(phen)Ni(*o*-Tol)Br **15**	−1.12[a]	
(phen*)NiBr$_2$ **17**	−0.69[b]	
(phen*)NiBr **18**		−1.37[b]
ZnBr$_2$ $E_{p/2}$(Zn^{II}/Zn)	−1.26[a]	

[a]In DMA at 25 °C, internal reference = Fc$^+$/Fc, electrolyte = Bu$_4$NBr. [b]In THF.

gives a Ni(I) species. The EPR spectra of **18** and **19** contain analogous features, which led us to assign the reduction intermediate **19** to (phen)Ni(I)Br. The EPR signal of this Ni-centered radical, however, only accounts for 10% of the Ni species. The loss of EPR signal could be attributed to the fast decomposition of the Ni(I) species or dimerization of **19**, as observed by Hazari and co-workers (eq 5).[7b] Previous studies

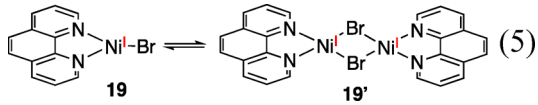

assign the reduced Ni species to Ni(0) in the presence of MgI$_2$.[5l] Further investigations into the salt effect on the redox potentials and their catalytic implications are essential and underway.

Stoichiometric Experiments To Probe Electrophile Activation. A solution of (phen)NiBr **19**, upon being generated in situ by reacting (phen)NiBr$_2$ **14** with Zn, was divided into two portions. In the presence of 2 equivalents of Zn, one solution of **19** was treated with 1 equivalent of PhBr, and the other with **11**. Monitoring both reactions by GC revealed that PhBr was consumed at a rate of 1.2 mM/min to form biphenyl, whereas the activation of **11** took place at a rate of 0.42 mM/min to afford dimer **20** (Figure 8). This kinetic comparison suggests that **19** reacts with PhBr faster than with **11**.

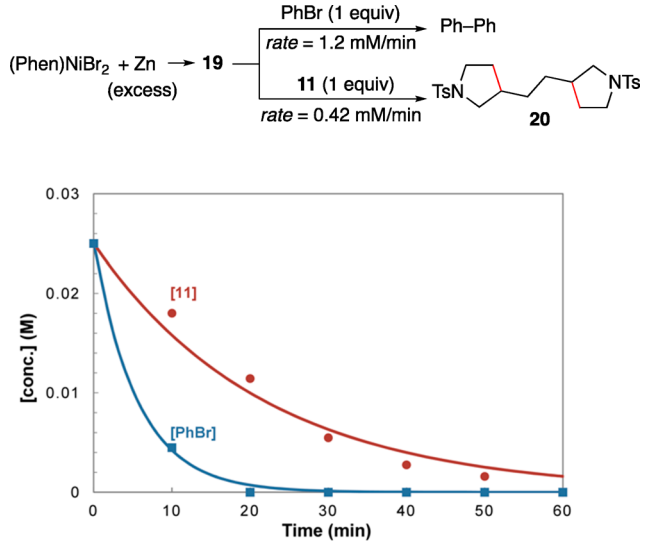

Figure 8. Kinetic comparison of PhBr with **11** in reacting with reduced Ni species **19**.

DOI: 10.1021/jacs.9b10026
J. Am. Chem. Soc. 2019, 141, 17937−17948

The purple solution of **19**, generated from the reduction of (phen)$NiBr_2$ by Zn, was filtered to remove excess Zn (eq 6).

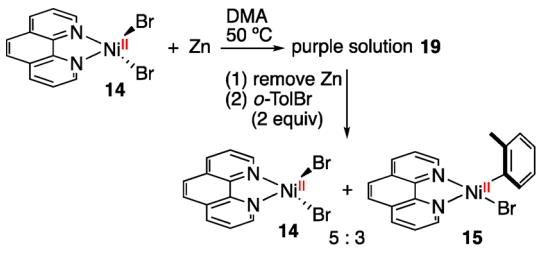

(6)

Addition of 2 equivalents of *o*-TolBr to this solution of **19** immediately forms (phen)$NiBr_2$ **14** and (phen)Ni(*o*-Tol)(Br) **15** in a ratio of 5:3, based on ^{1}H NMR analyses (Figures S20–S22).

The activation of PhBr by (phen)Ni(I)−Br **19** is faster than that of alkyl bromide **11**, which is evident from the comparison experiment shown in Figure 8. Results of eq 6 reveal that the activation of PhBr by (phen)Ni(I)−Br proceeds via a bimolecular oxidative addition to give **14** and **15**. Although the precise mechanism is unknown, this step may proceed via oxidative addition of *o*-TolBr to **19** followed by comproportionation of Ni(III) with another molecule of **19**. The observed ratio of **14** to **15** is greater than 1 (eq 6), and could be attributed to partial decomposition of **19** in the absence of Zn after filtration.

The formation of **15** from the reaction of **19** with *o*-TolBr prompted us to probe how possible intermediates, (phen)Ni(II)(*o*-Tol)(Br) **15** and (phen)Ni(Mes)(Br) **21** (Mes = 2,4,6-mesityl), interact with substrate **11**. Treating **15** with 1 equivalent of **11** at 50 °C forms **12** in 21% yield and dimer **20** in 4% yield (entry 1, Table 2). Reducing of **15** by Zn, followed by removal of Zn via filtration, generates a purple solution, which reacted with **11** to afford **12** in 37% yield and **20** in 12% yield (entry 2). Full conversion of **11** to **12** and **20** was achieved when Zn was retained in the reaction (entry 3). Complex **21** was inert toward **11** in the absence of Zn (entry 4). The reduction of complex **21** by Zn, followed by overnight treatment with **11**, led to 30% conversion of **11** to form **20** (entry 5).

Table 2. Stoichiometric Reaction of 15 and 21 with 11[a]

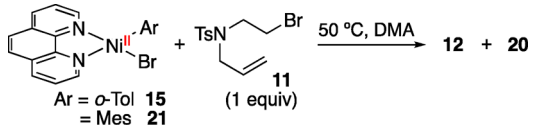

entry	Ar	Zn (equiv)	reaction time (h)	**11** (%)	**12** (%)	**20** (%)
1	*o*-Tol	0	2	70	21	4
2	*o*-Tol	2[b]	2	50	37	12
3	*o*-Tol	2	2	0	50	50
4	Mes	0	12	100	0	0
5	Mes	2[b]	12	69	0	30

[a]Yields were determined by ^{1}H NMR spectroscopy with 1,3,5-trimethoxylbenzene as the internal standard. [b]Zn was removed by filtration before addition of **11**.

Stoichiometric experiments between **15** and **11** suggest that **15** is capable of activating **11**, but the rate of this background reaction is exceeded by treating **11** with the reduced Ni species. The formation of dimer **20** implies a radical intermediate that undergoes cyclization and dimerization. The cross-coupling product **12** arises from the capture of the radical by Ni followed by reductive elimination. We attribute the incomplete conversion of **11** in entry 2 to the instability of the reduced Ni intermediate that underwent unproductive disproportionation in the absence of Zn after filtration. The more sterically hindered **21** suppressed the background activation of **11**. The radical intermediate, formed from activation of **11** by the reduced **21**, is hampered from binding to the Ni center sterically. Therefore, **20** is formed exclusively.

Characterization of the Reduction of (phen)Ni(Ar)(Br) by Zn. EPR analysis has shed light on the reduction of (phen)Ni(Mes)(Br) **21** by Zn. The dark red solution of (Phen)Ni(Mes)(Br) **21** was allowed to stir with Zn to afford a purple solution. The EPR spectrum of a frozen sample was recorded to give an isotropic signal with a *g* value of 2.009 (Figure 9). Treating (phen)Ni(I)−Br **19** with MesMgBr also afforded a purple solution with an analogous isotropic EPR spectrum (Figure S63). In contrast, transmetalation of MesMgBr to (phen*)Ni(I)−Br **18** gave a rhombic EPR signal with *g* values of 2.530, 2.141, and 2.058 (Figure S64).

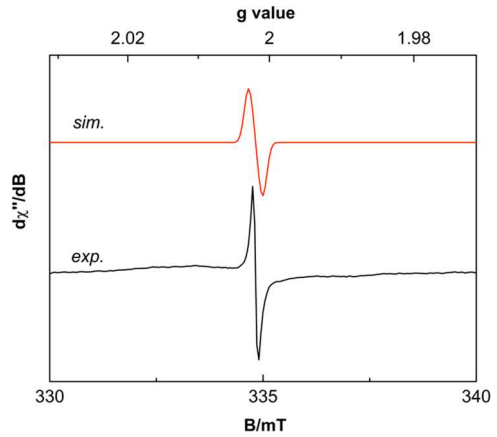

Figure 9. X-Band EPR spectrum of reduction reaction mixture of **21** with Zn. Temperature = 10 K, solvent = DMA. The spectrum is simulated with Easyspin. Spectroscopic parameters: *g* = 2.009. Microwave frequency = 9.380 GHz, power = 0.63 mW, modulation amplitude = 1 mT/100 kHz.

Yakhvarov and co-workers have electrochemically generated (phen)Ni(Mes) **25**, which shows an organic centered radical in its EPR spectrum.[26] This electronic structure has been attributed to the spin-tautomer **25′**, in which the redox-active phen delocalizes the electron to its π^* orbital to give a Ni(II) center and an organic radical (Scheme 3). Similar redox activity has been observed and characterized in (bpy)Ni-

Scheme 3. Proposed Ni(I) Species upon Reduction of 21 by Zn

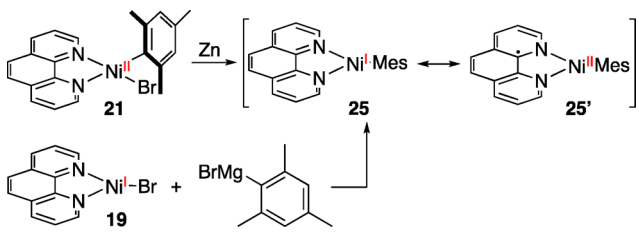

DOI: 10.1021/jacs.9b10026
J. Am. Chem. Soc. 2019, 141, 17937−17948

(Mes)[27] and (terpy)Ni(Mes) complexes.[28] The EPR spectrum of the reduction mixture of **21** by Zn displays an isotropic signal with a *g* value of 2.009, close to the free-electron value of 2.0023 (Figure 9). This observation indicates the ligand character of the SOMO, consistent with the previous characterization of (phen)Ni(Mes) **25**. The assignment of **25** has found support in the analogous EPR spectrum obtained from transmetalation of MesMgBr to **19** (Figure S63). In contrast, transmetalation of MesMgBr to **18** generates a Ni-centered radical. We assign this species to (phen*)Ni(Mes), based on the the data reported by Hazari.[7b] The different electronic structures between (phen)Ni(Mes) **25** and (phen*)Ni(Mes) could be attributed to the electron-donating effect of the *sec*-butyl substituents. Further research is underway to verify this hypothesis.

Radical Clock Cyclization As a Function of [Ni]. In the original method development, we reported that substrates undergoing slower radical cyclization give direct coupling product without cyclization.[10] We evaluated the product distribution as a function of [Ni]. Substrate **22** couples with PhBr to afford a mixture of **23**, derived from the direct coupling of alkyl bromide to PhBr, and the six-membered ring product **24** (Figure 10). Varying [Ni] resulted in a linear

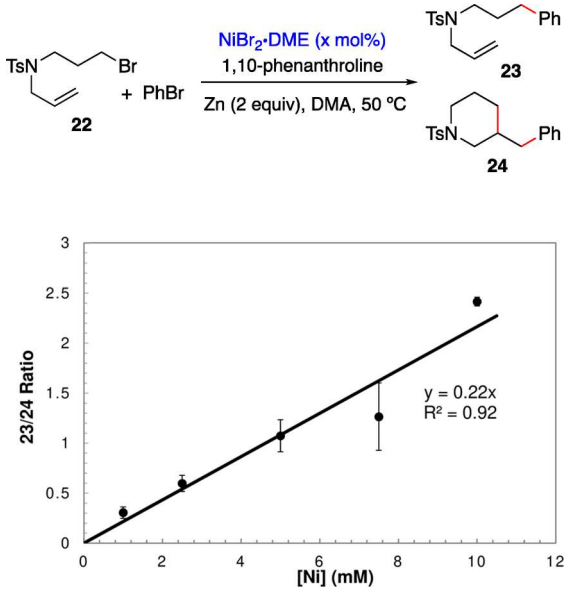

Figure 10. Ratio of uncyclized/cyclized products (**23**/**24**) as a function of [Ni] in the coupling of **22** with PhBr. Reaction conditions: $[\mathbf{22}]_0$ = 0.05 M, $[\mathrm{PhBr}]_0$ = 0.1−0.2 M, Zn = 0.1 mmol, solvent = DMA, agitation rate = 900 rpm, [(phen)$NiBr_2$·DME] = 1, 2.5, 5, 7.5, 10 mM. Data reflect the average of three independent trials.

increase in the ratio of **23**/**24** with a slope of 0.22. The linear dependence of the ratio of **23**/**24** on [Ni] resembles the observations by Hu[5d] and Weix[5e] in reactions going through free radical intermediates, but contrasts with the direct transmetalation mechanism, reported by Shenvi, when the group transfer occurs in the solvent cage.[5k]

Control Experiments. Zn is known to activate alkyl halides (particularly alkyl iodides) to form organozinc species.[29] We performed control experiments to verify whether bromo-alkene substrates could be activated with Zn in the absence of Ni. In the absence of Ni catalysts, heating Zn with **1** or **11** both led to decomposition of a small portion of the substrates without formation of any reduction products or carbocycles (eqs 7 and 8). These control experiments and the absence of carbocyle products reveal that alkyl bromide substrates must be activated by the Ni catalysts.

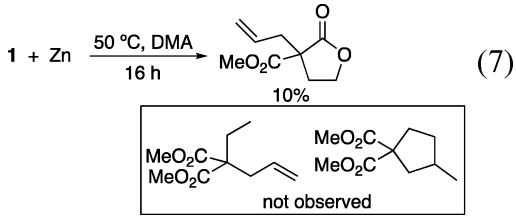

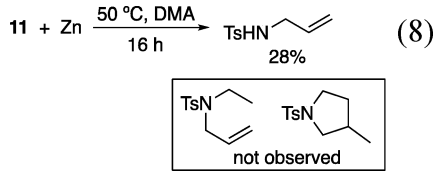

Evaluation of Mechanisms (A) and (B). Collectively, the kinetic data reveal that the rate of reductive 1,2-dicarbofunctionalization is independent of substrate concentration, and the turnover-limiting step is the reduction of Ni by Zn. Spectroscopic characterization identifies a mixture of (phen)-$NiBr_2$ and (phen)Ni(Ar)(Br) as the catalyst resting-state. Stoichiometric studies suggest that the reduction of Ni(II) complexes by Zn generates (phen)Ni(I)Br. (Phen)Ni(I)Br activates PhBr more rapidly than alkyl bromides via a bimolecular oxidative addition. EPR spectroscopy characterizes the reduction of (phen)Ni(Ar)(Br) by Zn to form (phen)Ni-(I)(Ar). The reaction of (phen)Ni(I)(Ar) with alkyl bromides generates radicals that can combine with Ni to form cross-coupling products.

"Radical chain" mechanisms (A) and (B) have been invoked in Ni-catalyzed cross-coupling and cross-electrophile coupling reactions (Scheme 1).[5] These pathways feature the activation of the alkyl bromide by (phen)Ni(I)−Br to form a radical (step i, Scheme 1), which combines with Ni(0) (step iii) or Ni(II) (step vii) species proceeding to further C−C bond formation. The kinetic comparison experiment shows that (phen)Ni(I)−Br activates PhBr more rapidly than alkyl bromides (Figure 8). This result contradicts with the activation of alkyl bromide by (phen)Ni(I)−Br in the "radical chain" mechanism (step i). In addition, kinetic and spectroscopic data suggest that the reduction of (phen)Ni(II) by Zn is the turnover-limiting step (Figures 2−5), with a rate constant of 8.6×10^{-4} s^{-1} at a 900 rpm agitation rate. Free alkyl radicals dimerize with a bimolecular rate constant on the order of 10^9 M^{-1} s^{-1}.[30] Drastically faster radical dimerization than Ni reduction by Zn suggests that the radical intermediate would not live long enough to be captured by (phen)Ni(0) if it is not the catalyst resting-state (pathway A, Scheme 1). In summary, the "radical chain" pathway is inconsistent with the kinetic data in this system.

Evaluation of Mechanism (C) and the Revised Mechanism. Our data support part of the "sequential reduction" mechanism shown in Scheme 1C, in which PhBr is activated prior to alkyl bromide. However, NMR, EPR, and CV characterizations of the reduction of (phen)$NiBr_2$ by Zn, and the comparison with model complex (phen*)NiBr **18**, establishes that Zn is only sufficient to reduce (phen)Ni(II)Br_2 **14** to (phen)Ni(I)Br **19**.[31] (Phen)Ni(0) is never formed under

DOI: 10.1021/jacs.9b10026
J. Am. Chem. Soc. 2019, 141, 17937−17948

these conditions. Accordingly, we revised the "sequential reduction" mechanism to exclude Ni(0) intermediates (Scheme 4).

Scheme 4. Revised Mechanism for Ni-Catalyzed Reductive 1,2-Dicarbofunctionalization of Alkenes

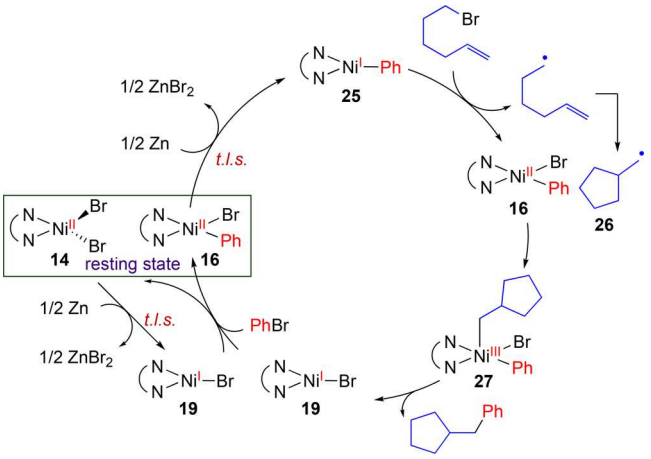

Stoichiometric experiments reveal that the activation of PhBr by (phen)Ni(I)Br **19** proceeds via bimolecular oxidative addition to generate (phen)$NiBr_2$ **14** and (phen)Ni(Ph)(Br) **16**. This step is reminiscent of previous reports on dinuclear Ni-mediated oxidative addition[5d,32] and reductive elimination.[33] (Phen)$NiBr_2$ **14** and (phen)Ni(Ph)(Br) **16** both exist as the catalyst resting-state. They are separately reduced by Zn to form **19** and **25** both as the turnover-limiting steps. The structures of **19** and **25** are assigned by comparing their EPR spectra with those of known analogous complexes. The reduction as the turnover-limiting step accounts for the lack of kinetic dependence on substrates and the observed kinetic dependence on the mixing speed and Zn loading (Figures 2 and 3), as well as the spectroscopic characterization of the catalyst resting-state (Figures 4 and 5).

(Phen)Ni(I)−Ph **25** can activate alkyl bromides to form radical intermediates. The presence of a radical intermediate is verified by stereochemical probes and radical clock substrates (Scheme 2). The reaction of **22** affords a mixture of the direct coupling product **23** and the cyclized product **24**; the ratio of **23**/**24**, which is proportional to the rate of step ii over the rate of step iv (Scheme 5), exhibits a linear correlation with [Ni]

Scheme 5. Proposed Mechanism for Forming 23 and 24 via a Radical Intermediate

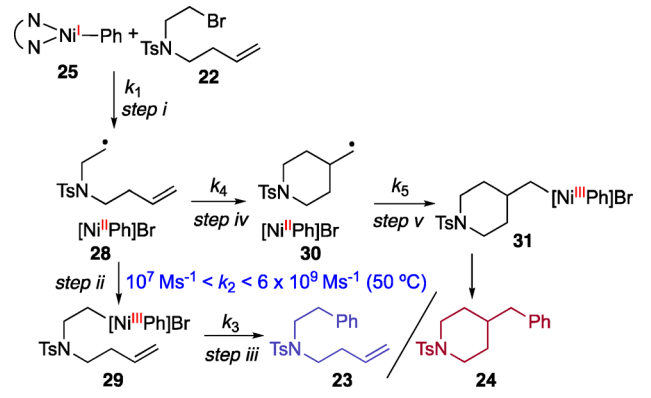

(Figure 10). Because radical cyclization is monomolecular (step iv), the linear correlation of **23**/**24** with [Ni] reflects a bimolecular process for radical coordination to Ni (step ii). On the basis of radical cyclization rates, we are able to estimate the range of radical capture rate by Ni(II) (k_4) to be higher than 10^7 M s^{-1} and lower than 6×10^9 M s^{-1} at 50 °C (see Supporting Information for the calculation),[34] which is consistent with the calculated barrier of 4 kcal/mol.[5g] Increasing the steric bulk of the ligand promotes the formation of dimer **4**, which can be attributed to a decreased radical trapping rate (Scheme 2A). Accordingly, substrates that would form seven-membered rings ($k_{cyclization}$ = 10^3 s^{-1}) underwent direct coupling with PhBr without cyclization.[10]

Selectivity for Activation of Electrophiles. Our data sheds light on the selectivity of cross-electrophile coupling reactions, which is a result of the different steric and electronic properties of Ni(I)−Br and Ni(I)−Ar intermediates. Csp^2 and Csp^3 electrophiles are independently activated by Ni(I)−Br and Ni(I)−Ar species, respectively, via distinct mechanisms (Scheme 6). Because oxidative addition of Csp^2−Br is most

Scheme 6. Illustration of Selectivity for Cross-Electrophile Coupling

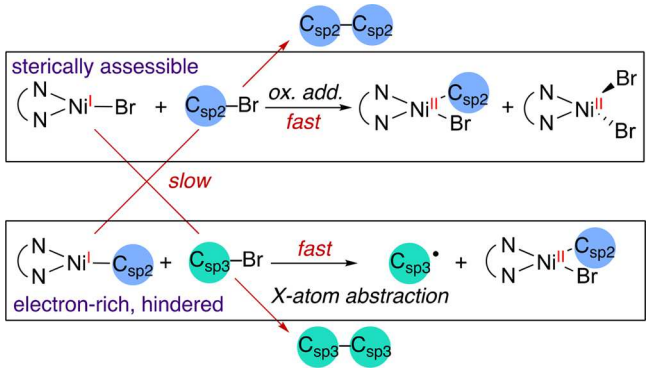

likely going through a two-electron, concerted pathway, the activation of Csp^2−Br is predominated by steric effects. (Phen)Ni(I)Br is sterically more accessible than (phen)Ni(I)-Ar; thus, it preferentially reacts with Csp^2−Br over Csp^3−Br. The activation of Csp^3−Br generates radicals via halogen-atom abstraction or single-electron transfer, and is most influenced by electronic effects. The electron-rich, yet sterically hindered (phen)Ni(I)Ar reacts with Csp^3−Br faster than with Csp^2−Br. An outcome of this kinetic preference is the selectivity achieved in cross-electrophile coupling over homo-coupling.

SUMMARY

The Ni-catalyzed two-component reductive dicarbofunctionalization of alkenes proceeds via a "sequential reduction" pathway. Kinetic data rules out the "radical chain" mechanism. Ni(I)−Br first activates ArBr to form Ni(II)(Br)(Ar), followed by subsequent reduction to a Ni(I)−Ar species. Ni(I)−Ar reacts with the alkyl bromide to form a radical that rapidly cyclizes and coordinates to Ni to afford a Ni(III) intermediate prior to reductive elimination. The key findings are (1) the turnover-limiting step is the reduction of Ni(II) by Zn, with Ni(II) species as the catalyst resting-state. This result highlights the importance of catalyst reduction. (2) Zn is only sufficient to reduce (phen)Ni(II) to (phen)Ni(I), and (phen)Ni(0) is absent from the reaction. (3) In the "sequential

DOI: 10.1021/jacs.9b10026
J. Am. Chem. Soc. 2019, 141, 17937−17948

reduction" pathway, two-electron, bimolecular oxidative addition of PhBr by (phen)Ni(I)−Br precedes the activation of alkyl bromides by (phen)Ni(I)−Ph via single-electron activation to give radicals. This sequence accounts for selectivity observed in cross-electrophile coupling reactions.

■ ASSOCIATED CONTENT

Supporting Information

The Supporting Information is available free of charge on the ACS Publications website at DOI: 10.1021/jacs.9b10026.

All experimental procedures, additional figures, details of DFT calculations, NMR spectra, and crystallographic data (PDF)

X-ray crystallographic data of **18** (CIF)

■ AUTHOR INFORMATION

Corresponding Author

*diao@nyu.edu

ORCID

Tianning Diao: 0000-0003-3916-8372

Notes

The authors declare no competing financial interest.

■ ACKNOWLEDGMENTS

We thank Professor Donna Blackmond for helpful discussions and suggestions and Chunhua (Tony) Hu for solving the X-ray crystal structure of complex **18**. Q.L. thanks Margalit Feuer for help with UV−vis measurements and Colin Anson (UW-Madison) for assistance with the EPR measurements. This work was supported by the National Institutes of Health (NIH) under award number 1R01GM127778. T.D. is a recipient of the Alfred P. Sloan Research Fellowship (FG-2018-10354) and the Camille-Dreyfus Teacher-Scholar Award (TC-19-019). T.D. acknowledges NSF (1827902) for funding to acquire an EPR spectrometer.

■ REFERENCES

(1) (a) Rosen, B. M.; Quasdorf, K. W.; Wilson, D. A.; Zhang, N.; Resmerita, A.-M.; Garg, N. K.; Percec, V. Nickel-Catalyzed Cross-Couplings Involving Carbon−Oxygen Bonds. *Chem. Rev.* **2011**, *111*, 1346. (b) Jahn, U. Radicals in Transition Metal Catalyzed Reactions? Transition Metal Catalyzed Radical Reactions: A Fruitful Interplay Anyway. In *Radicals in Synthesis III*; Heinrich, M., Gansäuer, A., Eds.; Springer: Berlin, Heidelberg, 2012; Vol. *320*, pp 323−451. (c) Tasker, S. Z.; Standley, E. A.; Jamison, T. F. Recent advances in homogeneous nickel catalysis. *Nature* **2014**, *509*, 299−309. (d) Cherney, A. H.; Kadunce, N. T.; Reisman, S. E. Enantioselective and Enantiospecific Transition-Metal-Catalyzed Cross-Coupling Reactions of Organometallic Reagents to Construct C−C Bonds. *Chem. Rev.* **2015**, *115*, 9587−9652. (e) Choi, J.; Fu, G. C. Transition metal−catalyzed alkyl-alkyl bond formation: Another dimension in cross-coupling chemistry. *Science* **2017**, *356*, eaaf7230. (f) Fu, G. C. Transition-Metal Catalysis of Nucleophilic Substitution Reactions: A Radical Alternative to SN1 and SN2 Processes. *ACS Cent. Sci.* **2017**, *3*, 692−700. (g) Lucas, E. L.; Jarvo, E. R. Stereospecific and stereoconvergent cross-couplings between alkyl electrophiles. *Nat. Rev. Chem.* **2017**, *1*, 0065.

(2) (a) Knappke, C. E. I.; Grupe, S.; Gärtner, D.; Corpet, M.; Gosmini, C.; Jacobi von Wangelin, A. Reductive Cross-Coupling Reactions between Two Electrophiles. *Chem. - Eur. J.* **2014**, *20*, 6828−6842. (b) Everson, D. A.; Weix, D. J. Cross-Electrophile Coupling: Principles of Reactivity and Selectivity. *J. Org. Chem.* **2014**, *79*, 4793−4798. (c) Weix, D. J. Methods and Mechanisms for Cross-Electrophile Coupling of Csp2 Halides with Alkyl Electrophiles. *Acc. Chem. Res.* **2015**, *48*, 1767−1775. (d) Gu, J.; Wang, X.; Xue, W.; Gong, H. Nickel-catalyzed reductive coupling of alkyl halides with other electrophiles: concept and mechanistic considerations. *Org. Chem. Front.* **2015**, *2*, 1411−1421. (e) Wang, X.; Dai, Y.; Gong, H. Nickel-Catalyzed Reductive Couplings. *Top. Curr. Chem.* **2016**, *374*, 43.

(3) (a) Hu, X. Nickel-catalyzed cross coupling of non-activated alkyl halides: a mechanistic perspective. *Chem. Sci.* **2011**, *2*, 1867. (b) Ananikov, V. P. Nickel: The "Spirited Horse" of Transition Metal Catalysis. *ACS Catal.* **2015**, *5*, 1964−1971. (c) Diccianni, J. B.; Diao, T. Mechanisms of Nickel-Catalyzed Cross-Coupling Reactions. *Trends in Chemistry* **2019**, DOI: 10.1016/j.trechm.2019.08.004.

(4) (a) Hegedus, L. S.; Miller, L. L. Reaction of.pi.-allylnickel bromide complexes with organic halides. Stereochemistry and mechanism. *J. Am. Chem. Soc.* **1975**, *97*, 459−460. (b) Tsou, T. T.; Kochi, J. K. Mechanism of biaryl synthesis with nickel complexes. *J. Am. Chem. Soc.* **1979**, *101*, 7547−7560. (c) Hegedus, L. S.; Thompson, D. H. P. The reactions of organic halides with (π-allyl)nickel halide complexes: a mechanistic study. *J. Am. Chem. Soc.* **1985**, *107*, 5663−5669. (d) Yamamoto, T.; Wakabayashi, S.; Osakada, K. Mechanism of C−C coupling reactions of aromatic halides, promoted by $Ni(COD)_2$ in the presence of 2,2′-bipyridine and PPh_3, to give biaryls. *J. Organomet. Chem.* **1992**, *428*, 223−237.

(5) (a) Jones, G. D.; Martin, J. L.; McFarland, C.; Allen, O. R.; Hall, R. E.; Haley, A. D.; Brandon, R. J.; Konovalova, T.; Desrochers, P. J.; Pulay, P.; Vicic, D. A. Ligand Redox Effects in the Synthesis, Electronic Structure, and Reactivity of an Alkyl−Alkyl Cross-Coupling Catalyst. *J. Am. Chem. Soc.* **2006**, *128*, 13175. (b) Lin, X.; Phillips, D. L. Density Functional Theory Studies of Negishi Alkyl−Alkyl Cross-Coupling Reactions Catalyzed by a Methylterpyridyl-Ni(I) Complex. *J. Org. Chem.* **2008**, *73*, 3680−3688. (c) Cornella, J.; Gómez-Bengoa, E.; Martin, R. Combined Experimental and Theoretical Study on the Reductive Cleavage of Inert C−O Bonds with Silanes: Ruling out a Classical Ni(0)/Ni(II) Catalytic Couple and Evidence for Ni(I) Intermediates. *J. Am. Chem. Soc.* **2013**, *135*, 1997−2009. (d) Breitenfeld, J.; Ruiz, J.; Wodrich, M. D.; Hu, X. Bimetallic Oxidative Addition Involving Radical Intermediates in Nickel-Catalyzed Alkyl−Alkyl Kumada Coupling Reactions. *J. Am. Chem. Soc.* **2013**, *135*, 12004−12012. (e) Biswas, S.; Weix, D. J. Mechanism and Selectivity in Nickel-Catalyzed Cross-Electrophile Coupling of Aryl Halides with Alkyl Halides. *J. Am. Chem. Soc.* **2013**, *135*, 16192−16197. (f) Schley, N. D.; Fu, G. C. Nickel-Catalyzed Negishi Arylations of Propargylic Bromides: A Mechanistic Investigation. *J. Am. Chem. Soc.* **2014**, *136*, 16588−16593. (g) Gutierrez, O.; Tellis, J. C.; Primer, D. N.; Molander, G. A.; Kozlowski, M. C. Nickel-Catalyzed Cross-Coupling of Photoredox-Generated Radicals: Uncovering a General Manifold for Stereoconvergence in Nickel-Catalyzed Cross-Couplings. *J. Am. Chem. Soc.* **2015**, *137*, 4896−4899. (h) Mohadjer Beromi, M.; Nova, A.; Balcells, D.; Brasacchio, A. M.; Brudvig, G. W.; Guard, L. M.; Hazari, N.; Vinyard, D. J. Mechanistic Study of an Improved Ni Precatalyst for Suzuki−Miyaura Reactions of Aryl Sulfamates: Understanding the Role of Ni(I) Species. *J. Am. Chem. Soc.* **2017**, *139*, 922−936. (i) Manzoor, A.; Wienefeld, P.; Baird, M. C.; Budzelaar, P. H. M. Catalysis of Cross-Coupling and Homocoupling Reactions of Aryl Halides Utilizing Ni(0), Ni(I), and Ni(II) Precursors; Ni(0) Compounds as the Probable Catalytic Species but Ni(I) Compounds as Intermediates and Products. *Organometallics* **2017**, *36*, 3508−3519. (j) Kc, S.; Dhungana, R. K.; Shrestha, B.; Thapa, S.; Khanal, N.; Basnet, P.; Lebrun, R. W.; Giri, R. Ni-Catalyzed Regioselective Alkylarylation of Vinylarenes via C(sp3)−C(sp3)/C(sp3)−C(sp2) Bond Formation and Mechanistic Studies. *J. Am. Chem. Soc.* **2018**, *140*, 9801−9805. (k) Shevick, S. L.; Obradors, C.; Shenvi, R. A. Mechanistic Interrogation of Co/Ni-Dual Catalyzed Hydroarylation. *J. Am. Chem. Soc.* **2018**, *140*, 12056−12068. (l) Wang, X.; Ma, G.; Peng, Y.; Pitsch, C. E.; Moll, B. J.; Ly, T. D.; Wang, X.; Gong, H. Ni-Catalyzed Reductive Coupling of Electron-Rich Aryl Iodides with Tertiary Alkyl Halides. *J. Am. Chem. Soc.* **2018**, *140*, 14490−14497. (m) Shu, W.; Garcia-Dominguez, A.; Quiros, M. T.; Mondal, R.; Cardenas, D. J.; Nevado, C. Ni-Catalyzed Reductive Dicarbofunctionalization of Nonactivated Alkenes: Scope and

Mechanistic Insights. *J. Am. Chem. Soc.* **2019**, *141*, 13812−13821. (n) Yin, H.; Fu, G. C. Mechanistic Investigation of Enantioconvergent Kumada Reactions of Racemic α-Bromoketones Catalyzed by a Nickel/Bis(oxazoline) Complex. *J. Am. Chem. Soc.* **2019**, *141*, 15433−15440.

(6) (a) Wang, S. C.; Troast, D. M.; Conda-Sheridan, M.; Zuo, G.; LaGarde, D.; Louie, J.; Tantillo, D. J. Mechanism of the Ni(0)-Catalyzed Vinylcyclopropane−Cyclopentene Rearrangement. *J. Org. Chem.* **2009**, *74*, 7822−7833. (b) Ritleng, V.; Henrion, M.; Chetcuti, M. J. Nickel N-Heterocyclic Carbene-Catalyzed C−Heteroatom Bond Formation, Reduction, and Oxidation: Reactions and Mechanistic Aspects. *ACS Catal.* **2016**, *6*, 890−906. (c) Diccianni, J. B.; Heitmann, T.; Diao, T. Nickel-Catalyzed Reductive Cycloisomerization of Enynes with CO_2. *J. Org. Chem.* **2017**, *82*, 6895−6903. (d) Chen, P. P.; Lucas, E. L.; Greene, M. A.; Zhang, S. Q.; Tollefson, E. J.; Erickson, L. W.; Taylor, B. L. H.; Jarvo, E. R.; Hong, X. A Unified Explanation for Chemoselectivity and Stereospecificity of Ni-Catalyzed Kumada and Cross-Electrophile Coupling Reactions of Benzylic Ethers: A Combined Computational and Experimental Study. *J. Am. Chem. Soc.* **2019**, *141*, 5835−5855.

(7) (a) Mohadjer Beromi, M.; Banerjee, G.; Brudvig, G. W.; Hazari, N.; Mercado, B. Q. Nickel(I) Aryl Species: Synthesis, Properties, and Catalytic Activity. *ACS Catal.* **2018**, *8*, 2526−2533. (b) Mohadjer Beromi, M.; Brudvig, G. W.; Hazari, N.; Lant, H. M. C.; Mercado, B. Q. Synthesis and Reactivity of Paramagnetic Nickel Polypyridyl Complexes Relevant to C(sp2)−C(sp3)Coupling Reactions. *Angew. Chem., Int. Ed.* **2019**, *58*, 6094−6098.

(8) Everson, D. A.; Jones, B. A.; Weix, D. J. Replacing Conventional Carbon Nucleophiles with Electrophiles: Nickel-Catalyzed Reductive Alkylation of Aryl Bromides and Chlorides. *J. Am. Chem. Soc.* **2012**, *134*, 6146−6159.

(9) (a) Kuang, Y.; Anthony, D.; Katigbak, J.; Marrucci, F.; Humagain, S.; Diao, T. Ni(I)-Catalyzed Reductive Cyclization of 1,6-Dienes: Mechanism-Controlled *trans* Selectivity. *Chem.* **2017**, *3*, 268−280. (b) Qin, X.; Lee, M. W. Y.; Zhou, J. S. Nickel-Catalyzed Asymmetric Reductive Heck Cyclization of Aryl Halides to Afford Indolines. *Angew. Chem., Int. Ed.* **2017**, *56*, 12723−12726. (c) He, Y.; Cai, Y.; Zhu, S. Mild and Regioselective Benzylic C−H Functionalization: Ni-Catalyzed Reductive Arylation of Remote and Proximal Olefins. *J. Am. Chem. Soc.* **2017**, *139*, 1061−1064. (d) García-Domínguez, A.; Li, Z.; Nevado, C. Nickel-Catalyzed Reductive Dicarbofunctionalization of Alkenes. *J. Am. Chem. Soc.* **2017**, *139*, 6835−6838. (e) Chen, F.; Chen, K.; Zhang, Y.; He, Y.; Wang, Y.-M.; Zhu, S. Remote Migratory Cross-Electrophile Coupling and Olefin Hydroarylation Reactions Enabled by in Situ Generation of NiH. *J. Am. Chem. Soc.* **2017**, *139*, 13929−13935. (f) Thapa, S.; Basnet, P.; Giri, R. Copper-Catalyzed Dicarbofunctionalization of Unactivated Olefins by Tandem Cyclization/Cross-Coupling. *J. Am. Chem. Soc.* **2017**, *139*, 5700−5703. (g) Qin, X.; Lee, M. W. Y.; Zhou, J. S. Nickel-Catalyzed Asymmetric Reductive Heck Cyclization of Aryl Halides to Afford Indolines. *Angew. Chem., Int. Ed.* **2017**, *56*, 12723−12726. (h) Wang, K.; Ding, Z.; Zhou, Z.; Kong, W. Ni-Catalyzed Enantioselective Reductive Diarylation of Activated Alkenes by Domino Cyclization/Cross-Coupling. *J. Am. Chem. Soc.* **2018**, *140*, 12364−12368. (i) Sun, S.-Z.; Börjesson, M.; Martin-Montero, R.; Martin, R. Site-Selective Ni-Catalyzed Reductive Coupling of α-Haloboranes with Unactivated Olefins. *J. Am. Chem. Soc.* **2018**, *140*, 12765−12769. (j) Zhao, X.; Tu, H. Y.; Guo, L.; Zhu, S.; Qing, F. L.; Chu, L. Intermolecular selective carboacylation of alkenes via nickel-catalyzed reductive radical relay. *Nat. Commun.* **2018**, *9*, 3488. (k) Anthony, D.; Lin, Q.; Baudet, J.; Diao, T. Nickel-Catalyzed Asymmetric Reductive Diarylation of Vinylarenes. *Angew. Chem., Int. Ed.* **2019**, *58*, 3198−3202. (l) Jin, Y.; Wang, C. Ni-catalyzed reductive arylalkylation of unactivated alkenes. *Chem. Sci.* **2019**, *10*, 1780−1785. (m) Tian, Z. X.; Qiao, J. B.; Xu, G. L.; Pang, X.; Qi, L.; Ma, W. Y.; Zhao, Z. Z.; Duan, J.; Du, Y. F.; Su, P.; Liu, X. Y.; Shu, X. Z. Highly Enantioselective Cross-Electrophile Aryl-Alkenylation of Unactivated Alkenes. *J. Am. Chem. Soc.* **2019**, *141*, 7637−7643.

(10) Kuang, Y.; Wang, X.; Anthony, D.; Diao, T. Ni-catalyzed two-component reductive dicarbofunctionalization of alkenes via radical cyclization. *Chem. Commun.* **2018**, *54*, 2558−2561.

(11) (a) Yu, X.; Yang, T.; Wang, S.; Xu, H.; Gong, H. Nickel-Catalyzed Reductive Cross-Coupling of Unactivated Alkyl Halides. *Org. Lett.* **2011**, *13*, 2138−2141. (b) Peng, Y.; Xu, X. B.; Xiao, J.; Wang, Y. W. Nickel-mediated stereocontrolled synthesis of spiroketals via tandem cyclization-coupling of beta-bromo ketals and aryl iodides. *Chem. Commun.* **2014**, *50*, 472−474. (c) Xiao, J.; Cong, X.-W.; Yang, G.-Z.; Wang, Y.-W.; Peng, Y. Divergent Asymmetric Syntheses of Podophyllotoxin and Related Family Members via Stereoselective Reductive Ni-Catalysis. *Org. Lett.* **2018**, *20*, 1651−1654.

(12) (a) Wang, X.; Liu, Y.; Martin, R. Ni-Catalyzed Divergent Cyclization/Carboxylation of Unactivated Primary and Secondary Alkyl Halides with CO_2. *J. Am. Chem. Soc.* **2015**, *137*, 6476−6479. (b) Zhang, Y.; Xu, X.; Zhu, S. Nickel-catalysed selective migratory hydrothiolation of alkenes and alkynes with thiols. *Nat. Commun.* **2019**, *10*, 1752−1761.

(13) (a) Cherney, A. H.; Kadunce, N. T.; Reisman, S. E. Catalytic Asymmetric Reductive Acyl Cross-Coupling: Synthesis of Enantioenriched Acyclic α,α-Disubstituted Ketones. *J. Am. Chem. Soc.* **2013**, *135*, 7442−7445. (b) Zhao, C.; Jia, X.; Wang, X.; Gong, H. Ni-Catalyzed Reductive Coupling of Alkyl Acids with Unactivated Tertiary Alkyl and Glycosyl Halides. *J. Am. Chem. Soc.* **2014**, *136*, 17645−17651.

(14) (a) Laskowski, C. A.; Bungum, D. J.; Baldwin, S. M.; Del Ciello, S. A.; Iluc, V. M.; Hillhouse, G. L. Synthesis and Reactivity of Two-Coordinate Ni(I) Alkyl and Aryl Complexes. *J. Am. Chem. Soc.* **2013**, *135*, 18272−18275. (b) Diccianni, J. B.; Katigbak, J.; Hu, C.; Diao, T. Mechanistic Characterization of (Xantphos)Ni(I)-Mediated Alkyl Bromide Activation: Oxidative Addition, Electron Transfer, or Halogen-Atom Abstraction. *J. Am. Chem. Soc.* **2019**, *141*, 1788−1796.

(15) Gibian, M. J.; Corley, R. C. Organic Radical-Radical Reactions - Disproportionation Vs Combination. *Chem. Rev.* **1973**, *73*, 441−464.

(16) RajanBabu, T. V. Stereochemistry of intramolecular free-radical cyclization reactions. *Acc. Chem. Res.* **1991**, *24*, 139.

(17) Yamago, S.; Matsumoto, A. Arylthiols as Highly Chemoselective and Environmentally Benign Radical Reducing Agents. *J. Org. Chem.* **2008**, *73*, 7300−7304.

(18) (a) Blackmond, D. G. Reaction Progress Kinetic Analysis: A Powerful Methodology for Mechanistic Studies of Complex Catalytic Reactions. *Angew. Chem., Int. Ed.* **2005**, *44*, 4302−4320. (b) Mathew, J. S.; Klussmann, M.; Iwamura, H.; Valera, F.; Futran, A.; Emanuelsson, E. A. C.; Blackmond, D. G. Investigations of Pd-Catalyzed ArX Coupling Reactions Informed by Reaction Progress Kinetic Analysis. *J. Org. Chem.* **2006**, *71*, 4711−4722.

(19) Burés, J. Variable Time Normalization Analysis: General Graphical Elucidation of Reaction Orders from Concentration Profiles. *Angew. Chem., Int. Ed.* **2016**, *55*, 16084−16087.

(20) Plata, R. E.; Hill, D. E.; Haines, B. E.; Musaev, D. G.; Chu, L.; Hickey, D. P.; Sigman, M. S.; Yu, J.-Q.; Blackmond, D. G. A Role for Pd(IV) in Catalytic Enantioselective C−H Functionalization with Monoprotected Amino Acid Ligands under Mild Conditions. *J. Am. Chem. Soc.* **2017**, *139*, 9238−9245.

(21) Charboneau, D. J.; Brudvig, G. W.; Hazari, N.; Lant, H. M. C.; Saydjari, A. K. Development of an Improved System for the Carboxylation of Aryl Halides through Mechanistic Studies. *ACS Catal.* **2019**, *9*, 3228−3241.

(22) Limousy, L.; Dutournie, P.; Hadjiev, D. Kinetics of Nitrite Reduction by Zinc Metal: Influence of Metal Shape on the Determination of Kinetic Parameters. *Water Environ. Res.* **2010**, *82*, 648−656.

(23) The relatively sharp resonances in (phen)$NiBr_2$ are not present in the reaction mixture, which we attribute to isomers formed from solvent coordination. The peaks converge in DMSO-d_6 (Figure S22).

(24) Jia, X.-G.; Guo, P.; Duan, J.; Shu, X.-Z. Dual nickel and Lewis acid catalysis for cross-electrophile coupling: the allylation of aryl halides with allylic alcohols. *Chem. Sci.* **2018**, *9*, 640−645.

DOI: 10.1021/jacs.9b10026
J. Am. Chem. Soc. 2019, 141, 17937−17948

(25) Neese, F. The ORCA Program System. *Wiley Interdisciplinary Reviews: Computational Molecular Science* **2012**, *2*, 73.
(26) Yakhvarov, D. G.; Petr, A.; Kataev, V.; Büchner, B.; Gómez-Ruiz, S.; Hey-Hawkins, E.; Kvashennikova, S. V.; Ganushevich, Y. S.; Morozov, V. I.; Sinyashin, O. G. Synthesis, structure and electrochemical properties of the organonickel complex [NiBr(Mes)(phen)] (Mes = 2,4,6-trimethylphenyl, phen = 1,10-phenanthroline). *J. Organomet. Chem.* **2014**, *750*, 59−64.
(27) Klein, A.; Kaiser, A.; Sarkar, B.; Wanner, M.; Fiedler, J. The Electrochemical Behaviour of Organonickel Complexes: Mono-, Di- and Trivalent Nickel. *Eur. J. Inorg. Chem.* **2007**, *2007*, 965−976.
(28) Hamacher, C.; Hurkes, N.; Kaiser, A.; Klein, A.; Schüren, A. Electrochemistry and Spectroscopy of Organometallic Terpyridine Nickel Complexes. *Inorg. Chem.* **2009**, *48*, 9947−9951.
(29) Knochel, P.; Singer, R. D. Preparation and reactions of polyfunctional organozinc reagents in organic synthesis. *Chem. Rev.* **1993**, *93*, 2117−2188.
(30) Ingold, K. U.; Adamic, K.; Bowman, D. F.; Gillan, T. Kinetic applications of electron paramagnetic resonance spectroscopy. I. Self-reactions of diethyl nitroxide radicals. *J. Am. Chem. Soc.* **1971**, *93*, 902−908.
(31) León, T.; Correa, A.; Martin, R. Ni-Catalyzed Direct Carboxylation of Benzyl Halides with CO_2. *J. Am. Chem. Soc.* **2013**, *135*, 1221−1224.
(32) Somerville, R. J.; Hale, L. V. A.; Gómez-Bengoa, E.; Burés, J.; Martin, R. Intermediacy of Ni−Ni Species in sp^2 C−O Bond Cleavage of Aryl Esters: Relevance in Catalytic C−Si Bond Formation. *J. Am. Chem. Soc.* **2018**, *140*, 8771−8780.
(33) (a) Zheng, B.; Tang, F.; Luo, J.; Schultz, J. W.; Rath, N. P.; Mirica, L. M. Organometallic Nickel(III) Complexes Relevant to Cross-Coupling and Carbon−Heteroatom Bond Formation Reactions. *J. Am. Chem. Soc.* **2014**, *136*, 6499−6504. (b) Xu, H.; Diccianni, J. B.; Katigbak, J.; Hu, C.; Zhang, Y.; Diao, T. Bimetallic C−C Bond-Forming Reductive Elimination from Nickel. *J. Am. Chem. Soc.* **2016**, *138*, 4779−4786. (c) Diccianni, J. B.; Hu, C.; Diao, T. N−N Bond Forming Reductive Elimination via a Mixed-Valent Nickel(II)−Nickel(III) Intermediate. *Angew. Chem., Int. Ed.* **2016**, *55*, 7534−7538. (d) Diccianni, J. B.; Hu, C.; Diao, T. Binuclear, High-Valent Nickel Complexes: Ni−Ni Bonds in Aryl−Halogen Bond Formation. *Angew. Chem., Int. Ed.* **2017**, *56*, 3635−3639.
(34) (a) Beckwith, A. L. J.; Moad, G. Intramolecular addition in hex-5-enyl, hept-6-enyl, and oct-7-enyl radicals. *J. Chem. Soc., Chem. Commun.* **1974**, 472−473. (b) Griller, D.; Ingold, K. U. Free-radical clocks. *Acc. Chem. Res.* **1980**, *13*, 317−323. (c) Newcomb, M. Radical Kinetics and Clocks. *Encyclopedia of Radicals in Chemistry, Biology and Materials* **2012**, 1 DOI: 10.1002/9781119953678.rad007.

DOI: 10.1021/jacs.9b10026
J. Am. Chem. Soc. 2019, 141, 17937−17948